Source of Acquisition
CASI Acquired

NACA

RESEARCH MEMORANDUM
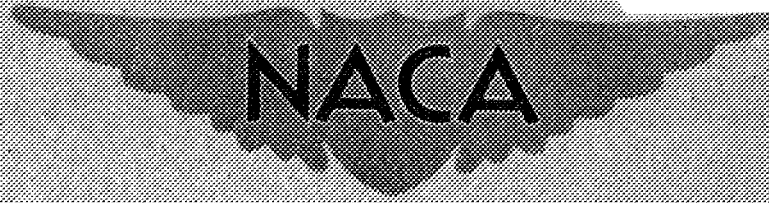
SPATIAL BURNOUT IN WATER REACTORS WITH NONUNIFORM

STARTUP DISTRIBUTIONS OF URANIUM AND BORON

By Thomas A. Fox and Donald Bogart

Lewis Flight Propulsion Laboratory
Cleveland, Ohio

RESTRICTED DATA

CLASSIFICATION CHANGE

To Unclassified

By authority of 01-TD-2724

Changed by M. Beda Date 3-11-74

This material contains information affecting the National Defense of the United States within the meaning of the espionage laws, Title 18, U.S.C., Secs. 793 and 794, the transmission or revelation of which in any manner to an unauthorized person is prohibited by law.

NATIONAL ADVISORY COMMITTEE
FOR AERONAUTICS
WASHINGTON

MAY 13 1955

~~CONFIDENTIAL~~ PRIORITY

NASA HEADQUARTERS

DEZ   6/7/72   9:00

EDWARD G. MAINES - SECURITY DIVISION   53356   X

NASA INSTALLATIONS
ATTN: SECURITY OFFICER

CONFIDENTIAL   NACA DOCUMENT RM E55C16, BY FOX AND BOGART WAS

ERRONEOUSLY LISTED AS UNCLASSIFIED BY HQS MEMO, 3/22/71, ITEM 7847

Restriction/Classification Cancelled   L. # 213-23.   IF REASONABLY

                                        RIBUTED ON UNCLASSIFIED

SSED TO CONFIDENTIAL R.D., GROUP L. ADVISE OF SITUATIONS WHERE

RECOVERY NOT FEASIBLE.

EDWARD G. MAINES
NASA SECURITY CLASSIFICATION OFFICER

DISTRIBUTION:
AMES RESEARCH CENTER
FLIGHT RESEARCH CENTER
GODDARD SPACE FLIGHT CENTER
KENNEDY SPACE CENTER
LANGLEY RESEARCH CENTER
LEWIS RESEARCH CENTER
MANNED SPACECRAFT CENTER
MARSHALL SPACE FLIGHT CENTER
NASA PASADENA OFFICE
WALLOPS STATION

cc: K55-10/RUDA

GROUP 4
...ed at 3 year

NATIONAL ADVISORY COMMITTEE FOR AERONAUTICS

RESEARCH MEMORANDUM

SPATIAL BURNOUT IN WATER REACTORS WITH NONUNIFORM STARTUP

DISTRIBUTIONS OF URANIUM AND BORON

By Thomas A. Fox and Donald Bogart

SUMMARY

Spatial burnout calculations have been made of two types of water moderated cylindrical reactor using boron as a burnable poison to increase reactor life. Specific reactors studied were a version of the Submarine Advanced Reactor (SAR) and a supercritical water reactor (SCW).

Burnout characteristics such as reactivity excursion, neutron-flux and heat-generation distributions, and uranium and boron distributions have been determined for core lives corresponding to a burnup of approximately 7 kilograms of fully enriched uranium. All reactivity calculations have been based on the actual nonuniform distribution of absorbers existing during intervals of core life. Spatial burnout of uranium and boron and spatial build-up of fission products and equilibrium xenon have been considered. Calculations were performed on the NACA nuclear reactor simulator using two-group diffusion theory.

The following reactor burnout characteristics have been demonstrated:

1. A significantly lower excursion in reactivity during core life may be obtained by nonuniform rather than uniform startup distribution of uranium. Results for SCW with uranium distributed to provide constant radial heat generation and a core life corresponding to a uranium burnup of 7 kilograms indicated a maximum excursion in reactivity of 2.5 percent. This compared to a maximum excursion of 4.2 percent obtained for the same core life when uranium was uniformly distributed at startup. Boron was incorporated uniformly in these cores at startup.

SECRET

2. It is possible to approach constant radial heat generation during the life of a cylindrical core by means of startup nonuniform radial and axial distributions of uranium and boron. Results for SCW with nonuniform radial distribution of uranium to provide constant radial heat generation at startup and with boron for longevity indicate relatively small departures from the initially constant radial heat generation distribution during core life. Results for SAR with a sinusoidal distribution rather than uniform axial distributions of boron indicate significant improvements in axial heat generation distribution during the greater part of core life.

3. Uranium investments for cylindrical reactors with nonuniform radial uranium distributions which provide constant radial heat generation per unit core volume are somewhat higher than for reactors with uniform uranium concentration at startup. On the other hand, uranium investments for reactors with axial boron distributions which approach constant axial heat generation are somewhat smaller than for reactors with uniform boron distributions at startup.

INTRODUCTION

The use of distributed burnable poisons in power reactors to achieve increased core life and to eliminate a large part of shim control has been under consideration for some time. Appropriate distribution of burnable poisons can permit fuel burnout to be balanced by poison burnout so as to maintain a reasonably small excursion in reactivity. The advantages of using burnable poisons in reactors required to maintain specified total power outputs were pointed out in reference 1. The application of burnable poisons to naval reactors was illustrated in reference 2 and its possibilities for increasing reactor life and simplifying control systems demonstrated. Reference 2 further suggested achievement of a more uniform heat flux and increased power densities by redistribution of the remaining core control rods present in a reactor such as the Submarine Thermal Reactor.

The principle of distributed burnable poisons is being applied in the design of the Submarine Advanced Reactor (SAR) by Knolls Atomic Power Laboratory (KAPL). In this connection NACA has cooperated with the Naval Reactors Branch of the Atomic Energy Commission and with KAPL in undertaking a study of achieving more uniform heat generation distributions in high specific-power reactors incorporating burnable poisons. In addition, the variation of reactivity with operating time at a fixed reactor power as affected by local axial or radial spatial burnout has been determined.

3542

CU-1 back

Because the use of distributed poison reduces the over-all amount of excess reactivity which is required to be controlled, it is possible that core control rods may be entirely replaced by control rods at the reflector-core interface. Removal of control rods from the core makes possible the achievement of more uniform power distributions by nonuniform startup distributions of uranium and poisons.

The present report presents the results of spatial burnout calculations for two cylindrical water reactors incorporating natural boron for longevity purposes. Several variations in startup axial and radial distributions of boron and uranium have been considered. The calculations have been performed on the NACA nuclear reactor simulator (ref. 3) using two-group diffusion theory.

REACTOR LONGEVITY CRITERIA

The use of burnable poisons to increase reactor life affects reactivity excursion and heat generation distribution. Reactor design criteria regarding nonuniform startup distributions of uranium and boron are discussed.

Reactivity excursion. - Because of the more rapid burnout of boron-10 relative to uranium-235, a reactor goes supercritical after startup. However, the loss in reactivity due to burnout of uranium-235 and accumulation of fission products results in the reactivity passing through a maximum. This excursion in reactivity must be compensated for by insertion of control rods or by reduction in reflector effectiveness during core life. A reactor longevity criterion is, therefore, to keep this excursion in reactivity to a minimum for a given burnable poison and specified core life.

The technique of "lumping" the burnable poison so that it shields itself at startup and makes available incremental quantities of poison as burnup proceeds has been considered in reference 4. It would seem possible by this means to flatten the reactivity excursion. In the present calculations, however, self-shielding effects have not been considered. What have been obtained are the burnout characteristics of a number of initially critical reactors with different spatially distributed concentrations of uranium-235 and boron-10 at startup. The initial investments were chosen so as to achieve a uranium burnup of about 7 kilograms; this corresponds to a gross heat generation of 133,000 megawatt hours.

Heat generation distribution. - Startup concentrations of uranium and boron are usually designed to be uniformly distributed in the reactor core. This would be conveniently obtained in practice by using identical uranium-boron elements equally spaced in the reactor core.

Heat generation distributions obtained for such reactors generally indicate peaks near the center of the core. These peaks, of course, seriously reduce the total power available from a reactor operating at limiting fuel-element temperature.

The objectionable peaks in heat generation can be removed by nonuniform distribution of uranium at startup. Techniques of initially achieving constant heat generation per unit core volume by nonuniform distribution of fissionable material are discussed in references 5 and 6. These techniques have been applied herein to indicate how a reactor designed for constant heat generation and incorporating a uniform concentration of burnable poison at startup is affected by spatial burnout.

Nonuniform startup distribution of burnable poison in the core can also improve the power distribution by altering relative spatial competition with uranium for available neutron flux. However, the higher neutron fluxes near the center of the core cause more rapid burnout of boron here than in the remainder of the core. The result is that during and at the end of core life, in reactors with initially uniform boron concentration, a significant quantity of boron remains in relative low flux regions. This serves only to increase uranium investment with no effect on reactor life.

Therefore a reactor longevity criterion for nonuniform boron distributions at startup is to produce (a) improvements in heat generation distribution and (b) savings in critical uranium investment as a result of smaller total quantities of boron necessary at startup to provide required core life.

SPECIFIC REACTORS

Submarine Advanced Reactor (SAR). - The first reactor considered corresponds to a version of SAR and consists of a cylindrical core 22 inches in diameter and 44 inches in height. It is cooled and moderated by water and contains stainless steel - zirconium fuel elements. The axial and radial reflectors are mixtures of water and stainless steel. Reactor specifications and nuclear constants used in the SAR calculations are given in table I(a). Nominal reactor power is specified at 65 megawatts and average reactor temperature at 575° F; a 7 kilogram uranium burnup would therefore correspond to a core life of 2000 hours.

Supercritical Water Reactor (SCW). - The second reactor considered is cooled and moderated by supercritical water. It consists of a cylindrical core 30 inches in diameter and 30 inches in height and contains stainless steel fuel elements. The axial and radial reflectors are assumed to be effectively infinite thicknesses of water. Reactor specifications and nuclear constants used in the SCW calculations are given

in table I(b). Nominal reactor power is specified at 300 megawatts, average reactor core temperature at 620° F, and average reflector temperature at 480° F. A 7 kilogram uranium burnup for this reactor would therefore correspond to a core life of about 450 hours.

REACTOR SPATIAL BURNOUT CALCULATIONS

For cylindrical reactors constructed of fuel elements running the height of the core, improvements in axial heat generation distributions may be more practically achieved from a fabricational viewpoint by a nonuniform axial distribution of burnable poison rather than uranium. However, in the radial direction, the possibility of using fuel elements with different uranium concentrations permits improvements in heat generation distributions by nonuniform radial distribution of uranium.

Cylindrical reactors incorporating the following distributions have been separately evaluated for the desired core life:

1. Nonuniform concentrations of boron and uniform concentrations of uranium in the axial direction for SAR.

2. Nonuniform concentrations of uranium and uniform concentrations of boron in the radial direction for SCW.

Spatial burnout characteristics such as reactivity excursion, core life, neutron flux, and heat generation distributions for the two water reactors have been calculated using two-group diffusion theory. The neutron diffusion equations, methods used for evaluating the two-group constants, and burnout relations are given in appendix B. (Symbols used are defined in appendix A.)

In order to achieve the desired uranium burnup of about 7 kilograms, the burnout characteristics of a number of initially critical reactors with different spatially distributed concentrations of uranium-235 and boron-10 have been obtained. Approximate startup compositions for these reactors were determined by homogeneous bare-pile calculations using assumed values of reflector savings (see appendix C). Reactivity excursion and core life for each reactor were determined by considering individual burnout periods which are successive intervals of the expected life of the reactor core. The spatial flux distribution and burnout characteristics were assumed to remain constant during each interval of the reactor life. Relatively long burnup intervals may be considered without loss in accuracy because heat generation and flux distributions change rather slowly with burnup as shown in appendix C. However, it is also shown in appendix C that longevity characteristics determined by homogeneous bare-pile calculations based on the variation with time of average rather than local core properties lead to serious inaccuracies.

Calculation Procedure

The reactivity calculations have been performed on the NACA nuclear reactor simulator. This electrical analog and the procedure for using it to solve reactor criticality problems have been described in references 3, 5, and 7. Although the reactor simulator employed is one-dimensional, solutions obtained include the effects of neutron leakage in the direction normal to the direction of solution. These effects are included by estimating reflector savings in this direction (see two-group equations in appendix B). Solutions obtained on the simulator automatically satisfy the required boundary conditions at the reactor center, core-reflector interface, and outer reflector boundary.

Absolute flux levels, required only for equilibrium xenon determination, were evaluated relative to the fluxes existing in the core at a position producing the nominal average power per unit core volume. Average equilibrium xenon concentration is approximately constant at these flux levels, so that the results obtained are applicable to wide ranges of total core power and reactor lifetime.

Both reactors considered are partly epithermal with 35 percent of the fissions for SAR and 20 percent of the fissions for SCW produced at energies above thermal at startup. Epithermal absorptions in uranium and their effects on thermal fluxes and equilibrium xenon concentrations have been considered in the simulator spatial burnout calculations within the limits of the two-group approach as outlined in reference 8.

Macroscopic cross sections and two-group parameters for a typical case of each reactor are given in table II. The uranium-235 and boron-10 concentrations listed are averages over the spatial distribution existing at the end of each individual burnup interval. Reactivity calculations, of course, were based on the actual nonuniform distribution of absorbers existing during intervals of core life. Spatial burnout of uranium and boron and spatial buildup of fission products and equilibrium xenon have been considered. Burnout relations used in computing spatial uranium and boron distributions are given in appendix B.

REACTOR BURNOUT CHARACTERISTICS

Spatial burnout characteristics of reactivity excursion, core life, and heat generation distribution determined for the axial direction for SAR and for the radial direction for SCW by the simulator spatial calculations are presented.

Reactivity Variation

The effective multiplication factor K_{eff} as a function of uranium-235 burnup is presented for both SAR and SCW in figure 1. (The circles indicate core burnup intervals considered.)

SAR. - Reactivity variations shown in figure 1(a) are for SAR with uniform axial distributions of boron and uranium at startup. Two cases with different initial investments of boron and uranium, SAR I and II, bracket the prescribed core life of 7 kilograms uranium burnup. Larger reactivity excursions accompany increased core life. A reactivity excursion of 2.5 percent was obtained for SAR II, which achieves closely the desired core life. This case required 30.0 kilograms of uranium-235 and 202 grams of natural boron at startup. Starting compositions, excursion, and burnup for all cases are summarized in table III. Excess reactivity requirements have not been considered.

Results in figure 1(b) are for SAR cases III and IV with uniform distributions of uranium and sinusoidal distributions of boron in the axial direction at startup. These startup boron distributions were chosen because they are proportional to the heat generation curve and so may be expected to approach uniform minimal concentrations of boron-10 at the end of core life. It will be seen later that a startup non-uniform boron distribution results in an improvement in heat generation distribution by flattening the axial neutron fluxes. There is also a savings in critical uranium investment because smaller quantities of boron are initially necessary to provide required core life.

The 202 grams of natural boron of SAR II were distributed sinusoidally in case SAR III. As shown in figure 1(b), a core uranium burnup of 8.1 kilograms was achieved. To obtain the required core life a fourth case, SAR IV, was computed in which the startup uranium investment was reduced to 27.3 kilograms and initial sinusoidally distributed boron requirement was reduced to 148 grams. SAR IV resulted in a core burnup of 6.4 kilograms so that the required burnup of 7 kilograms is bracketed. The reactivity excursion for the required burnup, interpolated from figure 1(b), is not affected by sinusoidal boron distribution in the axial direction.

Results for SAR IV indicate that required reactor life may be obtained by nonuniform axial distribution of boron using less boron and less uranium and with about the same excursion in reactivity as in the uniformly distributed boron case.

SCW. - The reactivity variations shown in figure 1(c) are for SCW with uniform radial distributions of boron and uranium at startup. Two cases, SCW I and II, were calculated. A reactivity excursion of 4.2 percent was obtained for SCW II for a 7 kilogram uranium burnup. The SCW core contains a lower concentration of uranium-235 than SAR so that

burnup of a given mass of uranium represents a larger fraction of the uranium concentration in SCW than in SAR. Inasmuch as the fractional boron-10 burnup is proportional to the fractional uranium-235 burnup raised to a power of 6.34 (see appendix B), boron-10 burns out more rapidly in SCW than in SAR and thus releases more excess reactivity after startup. SCW II required 25.1 kilograms of uranium-235 and 251 grams of natural boron at startup.

Results in figure 1(d) are for SCW III in which boron is uniformly distributed and uranium-235 is distributed radially in nonuniform concentrations so as to produce constant radial heat generation. SCW III required a critical mass of 29.5 kilograms of uranium and 217 grams of natural boron at startup. SCW III achieved a core burnup of 6.6 kilograms of uranium-235 and a maximum reactivity excursion of 2.5 percent. The heat generation distribution for this case is practically uniform throughout core life as will be presently seen.

Results for SCW III indicated that required reactor life may be obtained by nonuniform radial distribution of uranium using somewhat higher uranium and lower boron investments and with a significantly lower excursion in reactivity than in the uniformly distributed uranium case.

Heat Generation Distribution

Heat generation distributions for representative SAR and SCW cases at startup and at end of core life are presented in figure 2. The ratio of local heat release to average heat release per unit core volume $H/\overline{H}$ is shown as a function of reactor axial height for SAR and as a function of reactor radius for SCW. The distributions gradually assume final shape as burnout proceeds.

SAR. - The distributions shown in figure 2(a) are for case SAR II and are representative of patterns obtained with uniform concentrations of uranium and boron at startup. A maximum-to-minimum heat release ratio of 2.8 at startup and 2.7 at end of core life are obtained. A sharp upturn in thermal flux at the core-reflector interface results in a large relative heat release ratio in the last few centimeters of core.

In figure 2(b) are shown the distributions for case SAR IV with uniform uranium and sinusoidal boron spatial concentrations at startup. These distributions are somewhat flatter than those obtained for the initially uniform boron cases. Maximum-to-minimum heat release ratios of 2.0 at startup and 2.5 at end of core life which are obtained indicate an improvement over SAR II. Most of the improvement occurs in the first half of core life. This improvement gradually decreases as the net effect of burnout of boron and uranium no longer tends to flatten thermal neutron fluxes.

SCW. - The distributions shown in figure 2(c) are for case SCW II and are again representative of patterns obtained with uniform concentrations of uranium and boron at startup. As in case SAR II, the distribution improves slightly as uranium burnup proceeds preferentially in regions of power peaks. The reduced relative uranium concentration causes reduced heat generation at these peak locations as burnout proceeds. A maximum-to-minimum heat release ratio of 2.3 at startup and 1.9 at end of core life are obtained. There is a sharp upturn in heat release ratio at the core-reflector interface region.

The heat distributions shown in figure 2(d) are for case SCW III where uranium has been spatially distributed so as to produce constant radial heat generation at startup. The boron concentration was uniform and identical to SCW I. The maximum-to-minimum heat release ratio is therefore 1.0 at startup. This ratio gradually changes to 1.2 by the end of core life. Thus, the radial heat generation distribution remains effectively constant throughout core life and no sharp power gradients are present.

Neutron Flux Distributions

SAR. - Two-group axial neutron flux distributions for case SAR IV operating at constant total power are shown in figure 3(a). The local fluxes relative to the average thermal flux at startup $\varphi/\overline{\varphi}_{th,0}$ are presented as a function of axial height above the reactor midplane. Operation at a constant total power during core life causes the thermal fluxes to rise in the core as burnup proceeds. The fluxes for sinusoidal axial boron distributions are somewhat flatter than the usual fluxes obtained with initial uniform concentrations of boron. The sharp upturn in thermal flux at the core-reflector interface results in a large power gradient here.

SCW. - Two-group radial neutron flux distributions for case SCW III operating at constant total power are shown in figure 3(b). For this case a constant radial heat generation is obtained by nonuniform radial distribution of uranium. These flux distributions are representative.

Uranium Distributions

Spatial distributions of uranium-235 for individual burnup intervals considered are presented in figure 3. Local uranium concentration relative to average concentration at startup $N^U/\overline{N}_0^U$ are shown for the axial direction for SAR and for the radial direction for SCW. Burnout relations used are given in appendix B.

SAR. - Axial uranium distributions for cases SAR II and IV are shown in figures 4(a) and (b), respectively. The uniform distribution at startup gradually assumes the final nonuniform distribution. Average values of uranium concentration over the core relative to startup concentration $N^U/\overline{N}^U_0$ are included for each burnout interval.

SCW. - Radial uranium distributions for cases SCW II and III are shown in figures 4(c) and (d), respectively. Distributions for SCW II in figure 4(c) are similar to those obtained for SAR. However, uranium distribution necessary to produce uniform power concentration at startup for SCW III, indicated in figure 4(d), retains its general shape during core life.

Boron Distributions

The corresponding spatial distributions of boron for the individual burnup intervals for both SAR and SCW are shown in figure 5. Local boron concentrations relative to average concentration at startup $N^B/\overline{N}^B_0$ are shown for the axial direction for SAR and for the radial direction for SCW. Burnout relations used are given in appendix B.

SAR. - The axial boron distribution for case SAR II with uniform concentration of boron at startup is shown in figure 5(a). Nonuniform spatial burnout of boron leads to the irregular distributions shown with significant amounts of boron remaining in the region of the core-reflector interface.

The axial boron distribution for case SAR IV with sinusoidally located concentrations of boron at startup is shown in figure 5(b). Boron burnout for this case proceeds at a much greater rate at the center of the reactor with the result that the initial sinusoidal distribution approaches a relatively uniform distribution at end of core life. As indicated previously, this results in more desirable power distributions and lower critical uranium requirements.

SCW. - Radial boron distributions for cases SCW II and III are shown in figures 5(c) and (d). Distributions obtained as burnout proceeds are similar to those obtained with SAR with uniform boron distribution at startup.

SAR V. - Results for the sinusoidal boron distributions for SAR suggested an inquiry into the extent to which it is possible to approach constant axial heat generation per unit core volume at startup by nonuniform distribution of boron. It is recognized that a constant rate of heat release axially is not the most desirable from an engineering

viewpoint, since it would be possible to extract larger total amounts of heat from a reactor operating at constant fuel-element temperature in the axial direction. It is also recognized that although constant heat release at startup may be approached by nonuniform boron disposition, the rapid burnout of boron results in a gradual departure from constant heat release toward the end of core life.

With these considerations in mind, boron was distributed axially so as to obtain an initially flat heat generation curve. For this case SAR V, the boron distribution necessary is shown in figure 6 with boron concentration effectively zero at the core-reflector interface. The resulting heat generation curve, also shown in figure 6, is flat except at the core-reflector interface. The critical uranium requirement for case SAR V is 55 kilograms and natural boron requirement is 620 grams, both considerably greater than requirements for cases SAR I to IV. The life of this core, which would be considerably greater than a burnup of 7 kilograms of uranium, has not been evaluated. The heat generation at the interface rises significantly because of the feed-in of thermal neutrons from the reflector. An effective boron curtain at the interface would be required to suppress thermal fluxes here which in turn would require greater amounts of uranium to maintain criticality. However, improvements in heat generation are possible with boron distributions intermediate between that of cases SAR IV and V.

CONCLUSIONS

From two-group spatial burnout calculations of two types of water moderated cylindrical reactor incorporating boron and uranium concentrations in uniform or nonuniform spatial distribution at startup, the following reactor burnout characteristics have been demonstrated for a given core life:

1. A significantly lower excursion in reactivity during core life may be obtained by nonuniform rather than uniform startup distribution of uranium. Results for a supercritical water reactor with uranium distributed to provide constant radial heat generation and a core life corresponding to a uranium burnup of 7 kilograms indicated a maximum excursion in reactivity of 2.5 percent. This compared to a maximum excursion of 4.2 percent obtained for the same core life when uranium was uniformly distributed at startup.

2. It is possible to approach constant radial heat generation during the life of a cylindrical core by means of startup nonuniform radial and axial distributions of uranium and boron. Results for a supercritical water reactor with nonuniform radial distribution of uranium to provide constant radial heat generation at startup and with boron for longevity indicate relatively small departures from the initially constant

radial heat generation distribution during core life. Results for a version of the Submarine Advanced Reactor with sinusoidal rather than uniform axial distributions of boron indicate significant improvements in axial heat generation distribution during the greater part of core life.

3. Uranium investments for cylindrical reactors with nonuniform radial uranium distributions which provide constant radial heat generation are somewhat higher than for reactors with uniform uranium concentration at startup. On the other hand, uranium investments for reactors with axial boron distributions which approach constant axial heat generation are somewhat smaller than for reactors with uniform boron concentration at startup. Considerable design latitude would seem to be available for meeting reactor heat generation and core life requirements through the use of nonuniform startup distributions of uranium and boron with approximately the same uranium investments as for reactors in which uranium and boron are uniformly distributed at startup.

Lewis Flight Propulsion Laboratory
    National Advisory Committee for Aeronautics
        Cleveland, Ohio, March 23, 1955

3542

APPENDIX A

SYMBOLS

The following symbols are used in this report:

B^2 buckling constant

K neutron multiplication constant

K_{eff} effective multiplication factor

L_f^2 mean-square slowing-down length for fast neutrons

L_{th}^2 mean-square thermal diffusion length

N atom concentration per unit volume

P total fissions per unit volume of reactor core

P_{th} fraction of neutrons absorbed thermally

t time

v neutron velocity

α ratio of radiative capture cross section to fission cross section

β fraction of total fissions/(cc)(sec) occurring thermally

λ_{TR} macroscopic transport mean free path

ν neutrons produced per fission

Σ macroscopic neutron cross section

σ microscopic neutron cross section

φ neutron flux

Subscripts:

A absorption process

F fission process

f fast neutron group

th thermal neutron group

APPENDIX B

DIFFUSION EQUATIONS AND BURNOUT RELATIONS

Two-group diffusion equations. - The two-group neutron-diffusion equations for the cylindrical reactor configurations considered are:

$$
\text{Core}
\begin{cases}
\nabla^2\varphi_f + \left[K_f(1 - p_{th}) - 1\right]\dfrac{\varphi_f}{L_f^2} + \dfrac{\lambda_{TR,th}}{\lambda_{TR,f}}\dfrac{K_{th}}{L_{th}^2}\varphi_{th} - B^2\varphi_f = 0 \\[2em]
\nabla^2\varphi_{th} - \dfrac{1}{L_{th}^2}\varphi_{th} + \dfrac{\lambda_{TR,f}}{\lambda_{TR,th}}\dfrac{p_{th}}{L_f^2}\varphi_f - B^2\varphi_{th} = 0
\end{cases}
$$

$$
\text{Reflector}
\begin{cases}
\nabla^2\varphi_f - \dfrac{1}{L_f^2}\varphi_f - B^2\varphi_f = 0 \\[2em]
\nabla^2\varphi_{th} - \dfrac{1}{L_{th}^2}\varphi_{th} + \dfrac{\lambda_{TR,f}}{\lambda_{TR,th}}\dfrac{p_{th}}{L_f^2}\varphi_f - B^2\varphi_{th} = 0
\end{cases}
$$

Axial solutions to these equations have been obtained for SAR and radial solutions have been obtained for SCW. Epithermal fissions are included and are considered to occur in the fast group. Leakage of neutrons in the direction normal to the direction of solution is also included by consideration of the buckling constant for the equivalent unreflected dimension in the normal direction. Solutions obtained on the electrical-analog nuclear reactor simulator automatically satisfy the usual boundary conditions at the core center, core-reflector interface, and outer reflector boundary.

The procedure for evaluating nuclear constants for use in the two-group equations is described in references 9 and 10. The procedure is briefly outlined as follows:

The fast group constants K_f, p_{th}, $\lambda_{TR,f}$ for core and reflector have been averaged from fission to thermal energies by the flux distribution in an infinite medium of the same composition according to the Fermi age slowing-down model. Dependence of this flux distribution on the fission spectrum is included.

For water, L_f^2 is based on the experimental value of 33 square centimeters at room temperature $(\rho = 1\ \text{gm/cc})$ and is taken as inversely proportional to the square of the water density at higher

water temperatures. Values of L_f^2 for the core and reflector were computed by the following expression given by KAPL for hydrogenous media:

$$L_f^2 = 33 \frac{(1 + V)^2}{(\rho + xV)^2}$$

where x is an equivalence factor which depends upon the particular metal used in conjunction with water, V is the metal-water volume ratio, and ρ is the density of water. The equivalence factors used were $x^{Zr} = 0.40$, and $x^{S.S.} = 0.38$. In cores where two metals were present, a weighted average was obtained for x based on the volumetric concentration of the metals.

The thermal group constants K_{th}, $\lambda_{TR,th}$, L_{th}^2 have been evaluated by weighting local values according to the Maxwellian distribution of neutron flux for the temperature. The local absorption cross sections of all reactor materials with the exception of xenon-135 are assumed to be inversely proportional to neutron velocity v.

By means of the method of reference 11, the effects of chemical binding of hydrogen in water have been considered in evaluating $\lambda_{TR,th}$. Experimental values of σ_S^H as measured for water are used to calculate local values of σ_{TR}^H. The quantity $\lambda_{TR,th}$ for the medium is then evaluated by weighting local values by the Maxwellian distribution of neutron flux.

Uranium-235 burnout. - Uranium burnup rate is given by

$$- \frac{dN^U}{dt} = \Sigma_{A,th}^U \varphi_{th} + \Sigma_{A,f}^U \varphi_f = \left(\Sigma_{F,th}^U \varphi_{th} \right) \frac{\sigma_{A,th}^U}{\sigma_{F,th}^U} + \left(\Sigma_{F,f}^U \varphi_f \right) \frac{\sigma_{A,f}^U}{\sigma_{F,th}^U}$$

$$= \beta P(1 + \alpha_{th}) + (1 - \beta)P(1 + \alpha_f)$$

or burnup is

$$N_0^U - N_t^U = \left[\beta(1 + \alpha_{th}) + (1 - \beta)(1 + \alpha_f) \right] Pt$$

In the present calculations, the core life was specified as that corresponding to a uranium burnup of 7 kilograms of uranium-235. As such, the final value of Pt corresponds to 133,000 megawatt hours. The assumption was made that the ratios of radiative capture to fission in uranium-235 for thermal and fast groups are equal, that is, $\alpha_{th} = \alpha_f$.

Boron-10 burnout. - Boron-10 burnup rate is given by

$$- \frac{dN^B}{dt} = \Sigma^B_{A,th}\varphi_{th} + \Sigma^B_{A,f}\varphi_f$$

with

$$\varphi_{th} = \frac{\beta P}{\Sigma^U_{F,th}}$$

$$\varphi_f = \frac{(1 - \beta)P}{\Sigma^U_{F,f}}$$

$$- \frac{dN^B}{dt} = \Sigma^B_{A,th} \frac{\beta P}{\Sigma^U_{F,th}} + \Sigma^B_{A,f} \frac{(1 - \beta)P}{\Sigma^U_{F,f}}$$

or

$$- \frac{dN^B}{N^B} = \left[\frac{\sigma^B_{A,th}}{\sigma^U_{F,th}} \beta + \frac{\sigma^B_{A,f}}{\sigma^U_{F,f}} (1 - \beta) \right] \frac{P}{N^U_t} dt$$

But

$$N^U_t = N^U_0 - \left[\beta(1 + \alpha_{th}) + (1 - \beta)(1 + \alpha_f) \right] Pt$$

Therefore

$$\frac{N^B_t}{N^B_0} = \left[\frac{N^U_t}{N^U_0} \right]^{\left\{ \frac{\dfrac{\sigma^B_{A,th}}{\sigma^U_{A,th}} \beta(1 + \alpha_{th}) + \dfrac{\sigma^B_{A,f}}{\sigma^U_{A,f}} (1 - \beta)(1 + \alpha_f)}{\beta(1 + \alpha_{th}) + (1 - \beta)(1 + \alpha_f)} \right\}}$$

In the present calculations, the assumption was made that the ratios of microscopic absorption cross sections for boron-10 and uranium-235 for thermal and fast groups are equal. With the further assumption that $\alpha_f = \alpha_{th}$, the exponent above reduces to $\sigma^B_{A,th}/\sigma^U_{A,th} = 6.34$.

Fission products other than xenon. - The fission products other than xenon have been combined. An average fission product with a thermal absorption cross section $\sigma^{FP}_{A,th}$ of 100 barns at 0.025 ev is assumed to be generated per fuel atom fissioned. Its cross section

is assumed to follow the $1/v$ law. Burnup of these fission products with reactor operating time is neglected. Fission product generation rate is given by

$$\frac{dN^{FP}}{dt} = \Sigma^U_{F,th}\varphi_{th} + \Sigma^U_{F,f}\varphi_f = \beta P + (1 - \beta)P$$

$$N^{FP}_t = Pt$$

Equilibrium xenon. - Equilibrium concentration of xenon-135 is given by

$$N^{Xe} = \frac{y^{Xe}P}{\lambda^{Xe} + \sigma^{Xe}_{A,th}\varphi_{th}} = \frac{y^{Xe}P}{\lambda^{Xe} + \dfrac{\sigma^{Xe}_{A,th}\beta P}{N^U \sigma^U_{F,th}}}$$

where

y^{Xe} yield per fission = 0.067

$\sigma^{Xe}_{A,th}$ average over Maxwellian for thermal group

λ^{Xe} decay constant = 2.1×10^{-5} per second

Epithermal burnup. - In order to evaluate two-group epithermal burnup of uranium-235 and boron-10 independently, the average values of α_f and $\sigma^B_{A,f}/\sigma^U_{A,f}$ for use in the burnup expressions must be known for the reactors considered. The assumptions that $\alpha_f = \alpha_{th}$ and $\sigma^B_{A,f}/\sigma^N_{A,f} = \sigma^B_{A,th}/\sigma^U_{A,th}$ made in the present calculations, were qualitatively checked using the Goertzel-Selengut model. Inasmuch as the Goertzel-Selengut model is a more appropriate slowing-down model for hydrogenous media, values of these fast parameters were obtained by this model for an infinite medium closely corresponding to case SAR I startup composition; average values over the epithermal region of $\alpha_f = 1.85\ \alpha_{th}$ and $\sigma^B_{A,f}/\sigma^U_{A,f} = 0.80\ \sigma^B_{A,th}/\sigma^U_{A,th}$ were calculated.

Use of these values in the burnup expressions indicates that uranium-235 burns out 4.5 percent faster than for the entirely thermal assumption and therefore boron-10 also burns out faster (for case SAR I at 2000 hours, boron-10 burnup is increased by 5.0 percent). The net effect on reactivity for case SAR I is estimated to make the reactor considering epithermal effects only 0.1 percent more reactive than the reactor calculated under the foregoing thermal assumptions.

APPENDIX C

HOMOGENEOUS BARE-PILE CALCULATIONS

The two-group criticality equation for a homogeneous bare reactor is given by

$$\frac{K_{th}p_{th}}{(1 + L_f^2 B^2)(1 + L_{th}^2 B^2)} + \frac{K_f(1 - p_{th})}{(1 + L_f^2 B^2)} = 1$$

where for cylindrical reactors

$$B^2 = B_r^2 + B_z^2 = \left(\frac{2.405}{R_B}\right)^2 + \left(\frac{\pi}{H_B}\right)^2$$

and

$$R_B = R_C + \text{reflector radial savings}$$

$$H_B = H_C + 2(\text{reflector axial savings})$$

Criticality calculations have been made using this equation and the radial and axial reflector savings specified in table I. These calculations served as a guide for the spatial burnout solutions in all cases except SCW III with uniform radial heat generation. For bare-pile calculations, burnouts were based on the fluxes in the average unit volume of the reactor core. Comparison of the variation of reactivity with uranium burnup for SAR I and II as calculated by bare pile and spatial burnup techniques is shown in figure 7. There is a significant difference between the values of K_{eff} for the two calculations.

A large part of the difference between the values of K_{eff} for the spatial burnout cases (calculated on the simulator) and the homogeneous bare-pile calculations (based on the fluxes in the average unit volume of the reactor core) shown in figure 7 is due to the procedure used in calculating the boron-10 burnup. Because boron-10 burnup is related to uranium-235 burnup raised to a power of 6.34, the actual boron-10 burnup is not the average uranium burnup raised to this power, but the sum of the local uranium burnups, each raised to this power. The last procedure always results in a smaller boron burnup or more boron left. Therefore, reactors calculated on the simulator are less reactive than reactors calculated by homogeneous bare-pile procedure.

To illustrate these effects, the average boron-10 concentration at a core burnup of 6.64 kilograms, designated $\overline{N}_t^B$, has been evaluated by the two methods. A comparison of K_{eff} as calculated on the simulator and by homogeneous bare-pile considerations is given in the following table:

Method of calculation	$\overline{N}_t^B$ $\left(\dfrac{atoms}{cc\ core}\right)$		K_{eff} (at time t)	
	SAR I	SAR II	SAR I	SAR II
Simulator	1.50×10^{18}	1.93×10^{18}	0.988	1.007
Homogeneous bare pile	1.29	1.70	1.000	1.015
Homogeneous bare pile with simulator $\overline{N}_t^B$	1.50	1.93	.995	1.011

The results in the table indicate that the difference in method of calculation of boron-10 accounts for about half of the difference in resultant values of K_{eff}. The remaining difference between the simulator and bare-pile values of K_{eff} is probably due to the actual spatial variation of the thermal absorbers considered in the simulator solution. It should be noted that the homogeneous bare-pile calculations give good values of K_{eff} for reactor cores having uniform concentrations of strong thermal absorbers. However, values of K_{eff} as determined by the two types of calculations differ considerably with more extreme variations in spatial concentrations of thermal absorbers. For example, in SCW III with large radial variation in uranium concentration, a homogeneous bare-pile calculation has little meaning.

As previously mentioned, the flux distribution at the start of each burnout interval was assumed to hold for the entire interval. To check the sensitivity of this assumption, the reactivity after a uranium burnup of 6.64 kilograms was evaluated on the simulator for SAR I and II applying the flux distribution at reactor startup for the entire burnup period. These values are separately indicated in figure 7 at a core burnup of 6.64 kilograms and agree very closely with the smaller burnup intervals. These results indicate that the starting nonuniform spatial flux distributions are little affected by burnout and that rather large burnout intervals may be considered with small loss of precision.

REFERENCES

1. Weinberg, Alvin M.: Some Aspects of Reactor Theory. Reactor Sci.
   and Tech., vol. 3, no. 4, TID-2008, Mar. 1953, pp. 109-119.

2. Radkowsky, Alvin: Application of Burnout Poisons to Naval Reactor
   Design. Reactor Sci. and Tech., vol. 2, no. 4, TID-2004, Dec.
   1952, pp. 177-181.

3. Spooner, Robert B.: Using a Reactor Simulator for Design Analysis.
   Nucleonics, vol. 12, no. 4, Apr. 1954, pp. 36-39.

4. Hurwitz, H., Jr., and Nims, J. B., Jr.: Report of the Physics Sec-
   tion for September, October, November 1952. KAPL-847, Knolls
   Atomic Power Lab., Feb. 26, 1953, pp. 35-57. (Contract No. W-31-
   109, Eng. 52.)

5. McCready, Robert R., Spooner, Robert B., and Valerino, Michael F.:
   Distribution of Fissionable Material in Thermal Reactors of Spheri-
   cal Geometry for Uniform Power Generation. NACA RM E52C11, 1952.

6. Balent, Ralph: Flat-flux Cores. Reactor Sci. and Tech., vol. 4, no.
   3, TID-2014, Sept. 1954, pp. 125-129.

7. Fieno, Daniel, Schneider, Harold, and Spooner, Robert B.: Lumped
   Reflector Parameters for Two-Group Reactor Calculations. Nucle-
   onics, vol. 11, no. 8, Aug. 1953, pp. 16-18.

8. Bogart, D., and Valerino, M. F.: Some Epithermal Effects on Criti-
   cality Requirements of Water-Moderated Reactors. Reactor Sci. and
   Tech., vol. 4, no. 3, TID-2014, Sept. 1954, pp. 107-114.

9. Bogart, Donald, and Valerino, Michael F.: The Sodium Hydroxide Re-
   actor: Effect of Reactor Variables on Criticality and Fuel-Element
   Temperature Requirements for Subsonic and Supersonic Aircraft Nu-
   clear Propulsion. NACA RM E52I19, 1952.

10. Bogart, Donald, and Soffer, Leonard: Criticality Survey of Hydrox-
    ides as Coolant Moderators for Aircraft Nuclear Reactors. NACA
    RM E53F30, 1953.

11. Radkowsky, A.: Temperature Dependence of Thermal Transport Mean
    Free Path. Quarterly Rep., Apr., May, June 1950. ANL-4476,
    Phys. Div., Argonne Nat. Lab., July 5, 1950, pp. 89-100. (Con-
    tract No. W-31-109, Eng. 38.)

TABLE I. - REACTOR SPECIFICATIONS AND CONSTANTS

(a) The Submarine Advanced Reactor (SAR)

$$\left[\begin{array}{l} T_{av} = 575^{\circ}\text{ F; } kT = 0.0495 \text{ ev; } u_{th} = 19.12 \\ \rho^{H_2O} = 0.731; \ \rho^{Zr} = 6.40; \ \rho^{SS\text{-}304} = 7.92. \end{array}\right]$$

Composition by volume			
Core (22-in. diam.; 44-in. height)	Axial reflector (10-in. thickness; 9-cm reflector saving)	Radial reflector (14-in. thickness; 12-cm reflector saving)	SS-304
H$_2$O 0.600 SS-304 .148 Zr .244 U .008 <u>1.000</u>	H$_2$O 0.900 SS-304 .100 <u>1.000</u>	H$_2$O 0.350 SS-304 .650 <u>1.000</u>	Cr 0.202 Ni .085 Fe .713 <u>1.000</u>

Atomic concentration, N, atoms/cc		
Atom	Core	Axial reflector
H O Zr Cr Ni Fe	0.02936×10^{24} .01468 .01034 .00258 .00109 .00911	0.04403×10^{24} .02201 .00174 .000734 .00616

Thermal cross sections ($u_{th} = 19.12$)						
Atom	Core				Axial reflector	
	σ_A, barns	σ_S, barns	Σ_A, 1/cm	Σ_{TR}, 1/cm	Σ_A, 1/cm	Σ_{TR}, 1/cm
H	.2246	[a]23.3 $\left(\sigma_{TR}^{H}\right)$	0.00584	0.6841	0.00877	1.0259
O	.0007	4.0	0	.0563	0	.0844
Zr	.2457	9.0	.00225	.0920		
Cr	2.037	4.2	.00466	.0107	.00314	.0072
Ni	3.151	17.3	.00303	.0186	.00205	.0125
Fe	1.678	10.9	.01354	.0978	.00915	.0661
U^{235}	446.8 380 $\left(\sigma_F^{U}\right)$	8.2	(b)	Negligible		
B^{10}	2830	4.0	(b)	Negligible		
Fission product	71.1	0	(b)	0		

[a]Averaged over Maxwellian including chemical binding effects.

[b]Varies with burnout.

TABLE I. - Concluded. REACTOR SPECIFICATIONS AND CONSTANTS

(b) The Supercritical Water Reactor (SCW)

Core: $T_{av} = 620^\circ$ F; $kT = 0.052$ ev; $u_{th} = 19.07$; $\rho^{H_2O} = 0.71$; $\rho^{SS\text{-}347} = 8.03$

Reflector: $T_{av} = 480^\circ$ F; $kT = 0.045$ ev; $u_{th} = 19.22$; $\rho^{H_2O} = 0.83$.

Composition by volume			
Core (30-in. diam; 30-in. height)	Axial reflector (Effectively infinite thickness; 7.5-cm reflector saving)	Radial reflector (Effectively infinite thickness; 7.5-cm reflector saving)	SS-347

H_2O 0.884
SS-347   .116
U   0
      1.000
	H_2O 1.000	H_2O 1.000	Fe 0.690
			Ni .085
			Cr .195
			Mn .021
			Nb .009
			    1.000

Atomic concentration, N, atoms/cc		
Atom	Core	Reflectors
H O Fe Ni Cr Mn Nb	0.04220×10^{24} .02110 .006854 .0009057 .001840 .0001933 .00005716	0.05552×10^{24} .02776

Core thermal cross sections ($u_{th} = 19.07$)				
Atom	σ_A, barns	σ_S, barns	Σ_A, 1/cm	Σ_{TR}, 1/cm
H	0.2195	[a]22.1	0.00926	0.935
O	.0007	4.0	Negligible	.0808
Fe	1.684	10.9	.01154	.0740
Ni	3.119	17.3	.00283	.0154
Cr	1.985	4.2	.00370	.0076
Mn	8.73	2.3	.00169	.0004
Nb	.762	5.0	.00004	.0003
U^{235}	440.0	8.2	(b)	Negligible
B^{10}	2760.0	4.0	(b)	Negligible
Fission product	69.3	0	(b)	0

[a]Averaged over Maxwellian including chemical binding effects.

[b]Varies with burnup.

TABLE II. - MACROSCOPIC CROSS SECTIONS AND PARAMETERS[a]

Parameter	SAR II					Axial reflector	SCW II						Radial reflector
	Burnup, kg U^{235}						Burnup, kg U^{235}						
	0	1.66	3.32	4.98	6.64		0	1.5	3.0	4.5	6.0	7.0	
$\lambda_{TR,f}$, cm	3.504	3.504	3.504	3.504	3.504	3.563	3.899	3.899	3.899	3.899	3.899	3.899	4.13
L_f^2, cm^2	92.4	92.4	92.4	92.4	92.4	69.5	67.5	67.5	67.5	67.5	67.5	67.5	47.9
$\lambda_{TR,th}$, cm	1.042	1.042	1.042	1.042	1.042	.836	.9180	.9180	.9180	.9180	.9180	.9180	.4747
P_{th}	.676	.694	.712	.727	.740	.950	.792	.808	.821	.832	.842	.848	.950
K_{th}	1.394	1.416	1.430	1.428	1.415	------	1.300	1.336	1.354	1.355	1.343	1.324	------
K_f	1.403	1.422	1.432	1.430	1.418	------	1.267	1.297	1.312	1.314	1.303	1.287	------
$\Sigma_{A,th}^{H_2O+SS}$, 1/cm	.02930	.02930	.02930	.02930	.02930	.02310	.02609	.02609	.02609	.02609	.02609	.02609	.01208
$\Sigma_{A,th}^{B^{10}}$, 1/cm	.02088	.01495	.01016	.00702	.00484		.02000	.01371	.00927	.00618	.00406	.00303	
$\Sigma_{A,th}^{U^{235}}$, 1/cm	.11083	.10469	.09855	.09242	.08628		.07382	.06943	.06504	.06065	.05626	.05307	
$\Sigma_{A,th}^{FP}$, 1/cm	0	.000831	.001662	.002492	.003323		0	.00051	.00102	.00153	.00204	.00238	
$\Sigma_{A,th}^{Xe}/\Sigma_{A,th}^{U}$, 1/cm	.0727	.0713	.0703	.0696	.0689		.0650	.06524	.05966	.05870	.05866	.05879	
$\Sigma_{A,th}^{Xe}$, 1/cm	.00806	.00746	.00693	.00643	.00595		.00480	.00453	.00388	.00356	.00330	.00312	
$N^{U^{235}} \cdot 10^{20}$, atoms/cc	2.800	2.645	2.490	2.335	2.180		1.890	1.780	1.665	1.555	1.440	1.360	
$N^{B^{10}} \cdot 10^{20}$, atoms/cc	.0833	.0597	.0406	.0280	.0193		.0818	.0561	.0379	.0253	.0166	.0124	
K_{eff}	1.000	1.019	1.025	1.020	1.007		1.000	1.026	1.040	1.040	1.022	1.001	

[a] Averaged over the nonuniform spatial distribution of absorbers existing at period of core life.

TABLE III. - INITIAL INVESTMENTS, MAXIMUM REACTIVITY EXCURSION AND

CORE LIFE FOR REACTOR CORES CONSIDERED

Case	Fully enriched U^{235} startup requirement, kg (a)	Natural boron startup requirement, g	Maximum excursion reactivity, percent	Reactor core life burnup of U^{235}, kg
SAR I	28.2	173	1.65	5.8
SAR II	30.0	202	2.50	7.2
SAR III	29.5	202	2.70	8.1
SAR IV	27.3	148	1.85	6.3
SAR V	55.0	620	----	---
SCW I	24.0	217	3.10	5.6
SCW II	25.1	251	4.18	7.0
SCW III	29.5	217	2.55	6.6

[a]Exclusive of excess reactivity requirements.
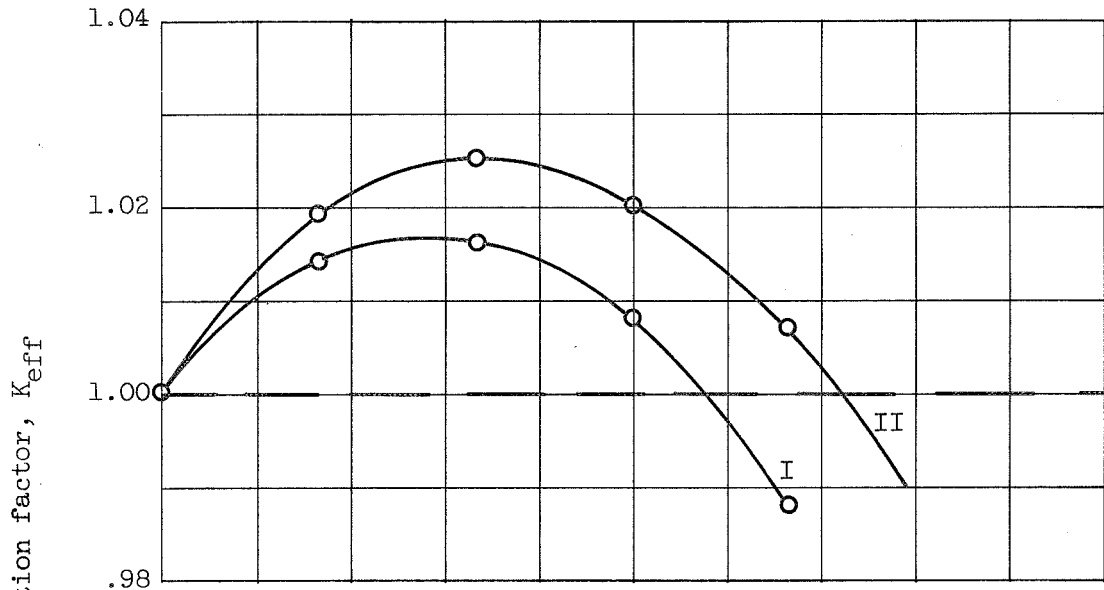
(a) Cases SAR I and II.
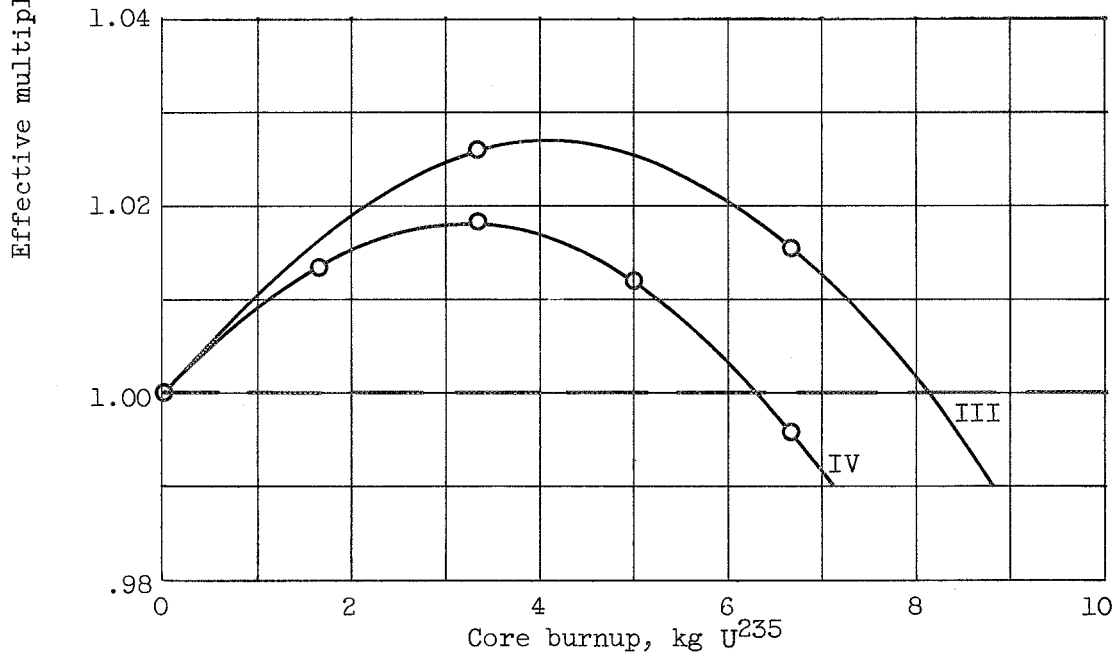
(b) Cases SAR III and IV.

Figure 1. - Reactivity variation with core uranium burnup.
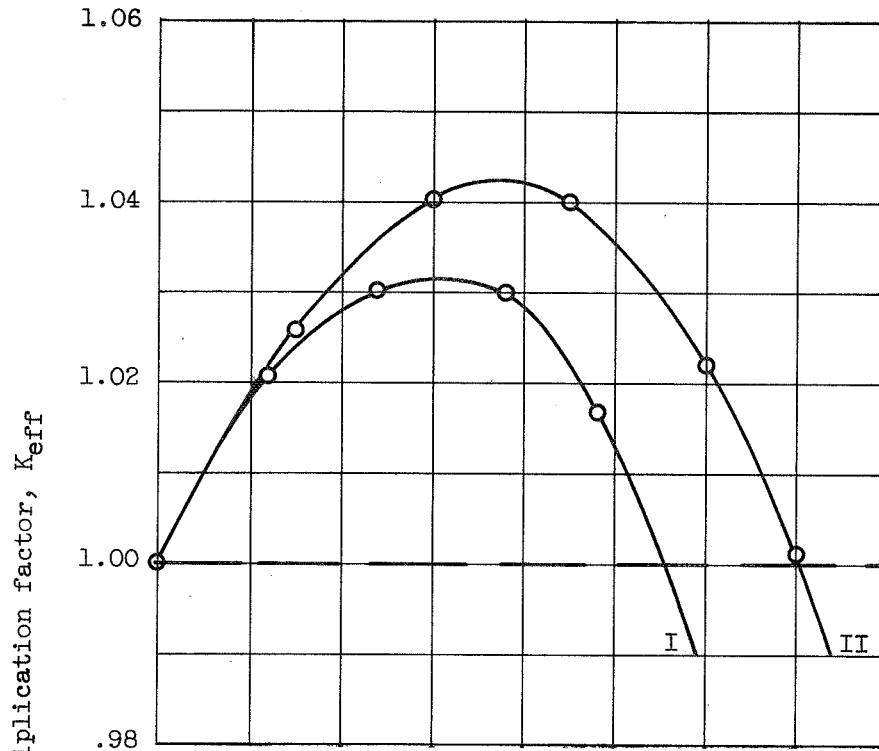
(c) Cases SCW I and II.
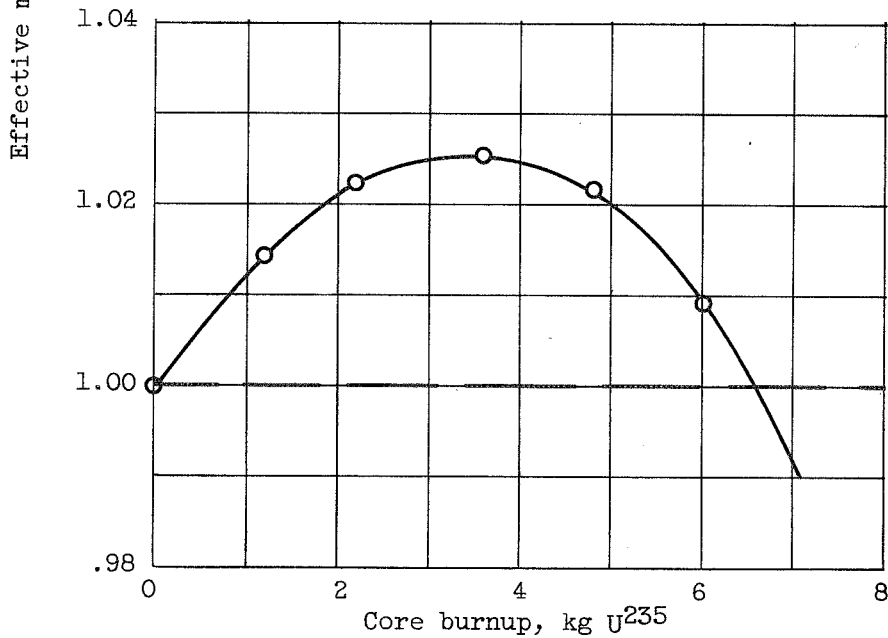
(d) Case SCW III.

Figure 1. - Concluded. Reactivity variation with
core uranium burnup.
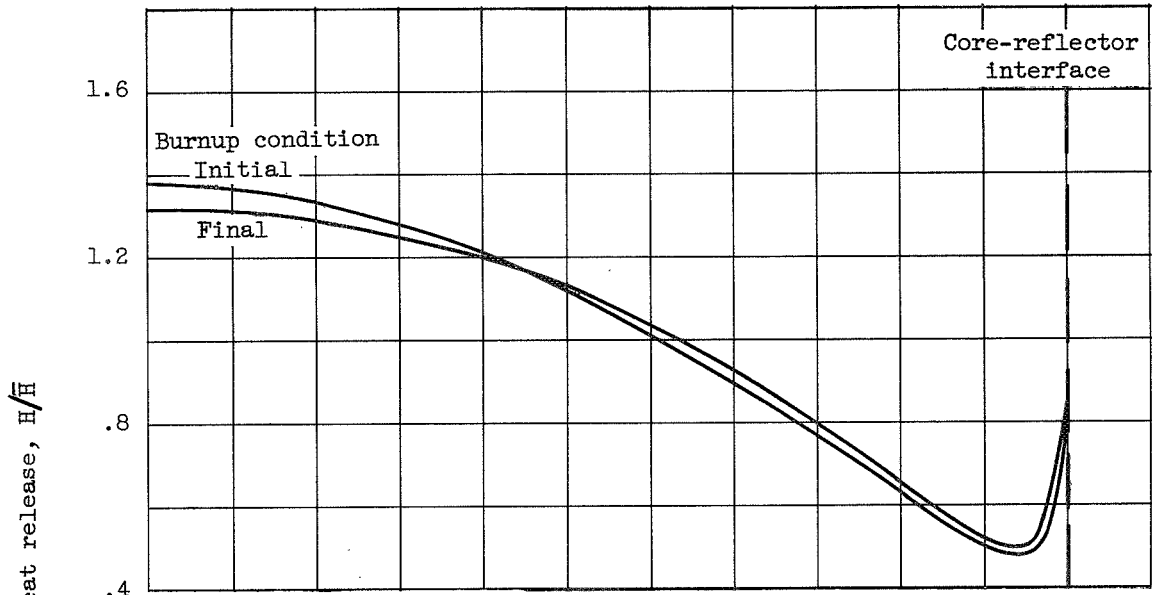
(a) Case SAR II.
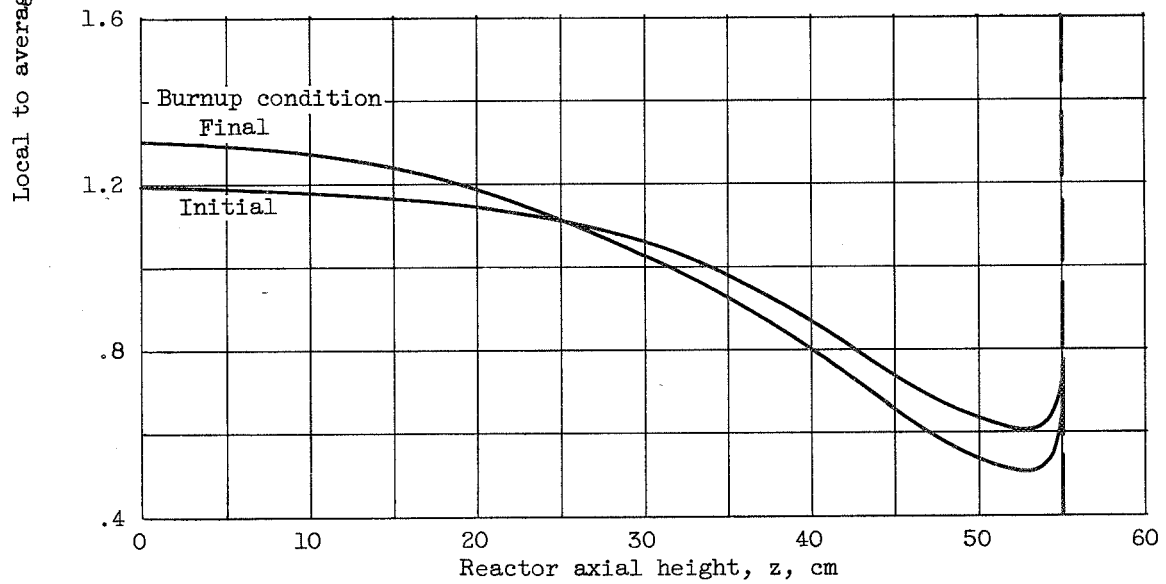
(b) Case SAR IV.

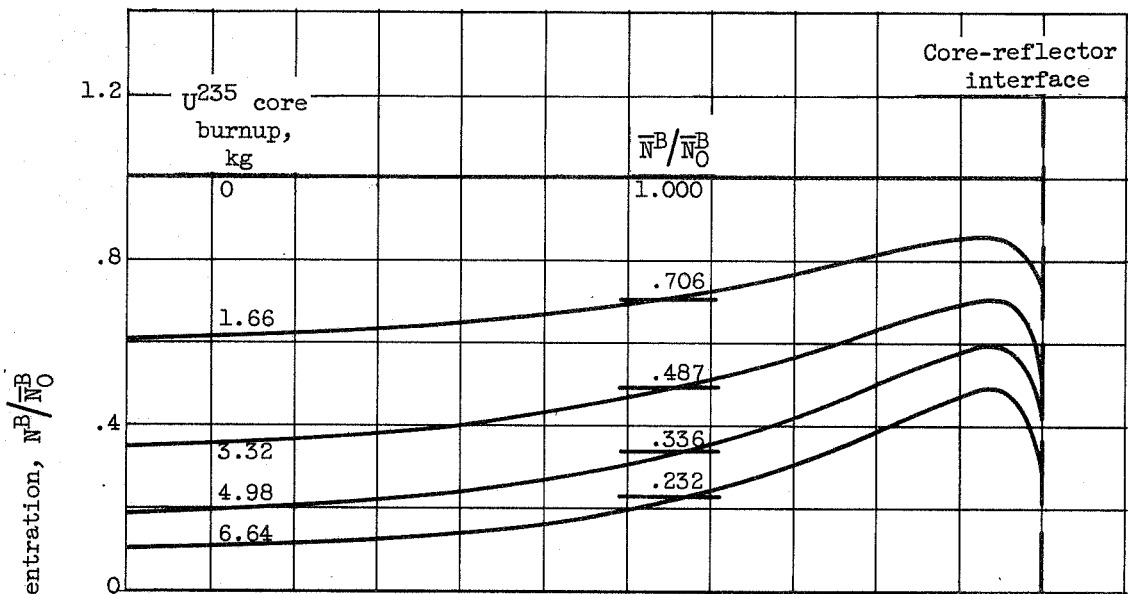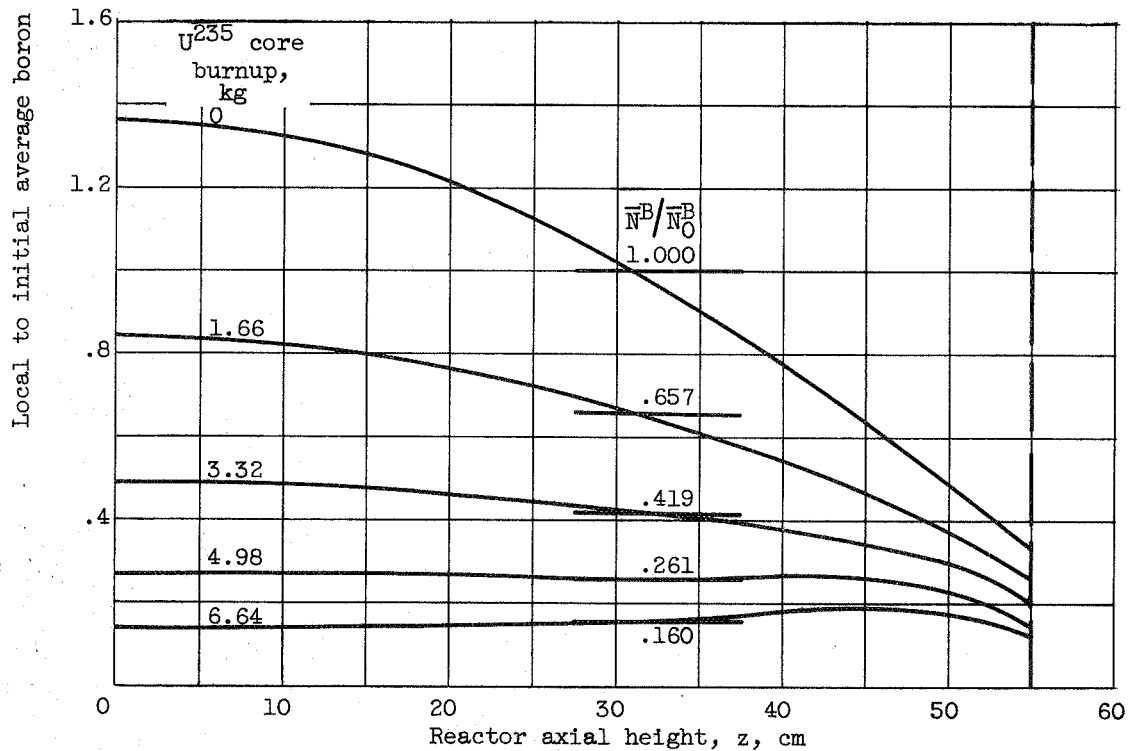Figure 2. - Heat generation distributions.
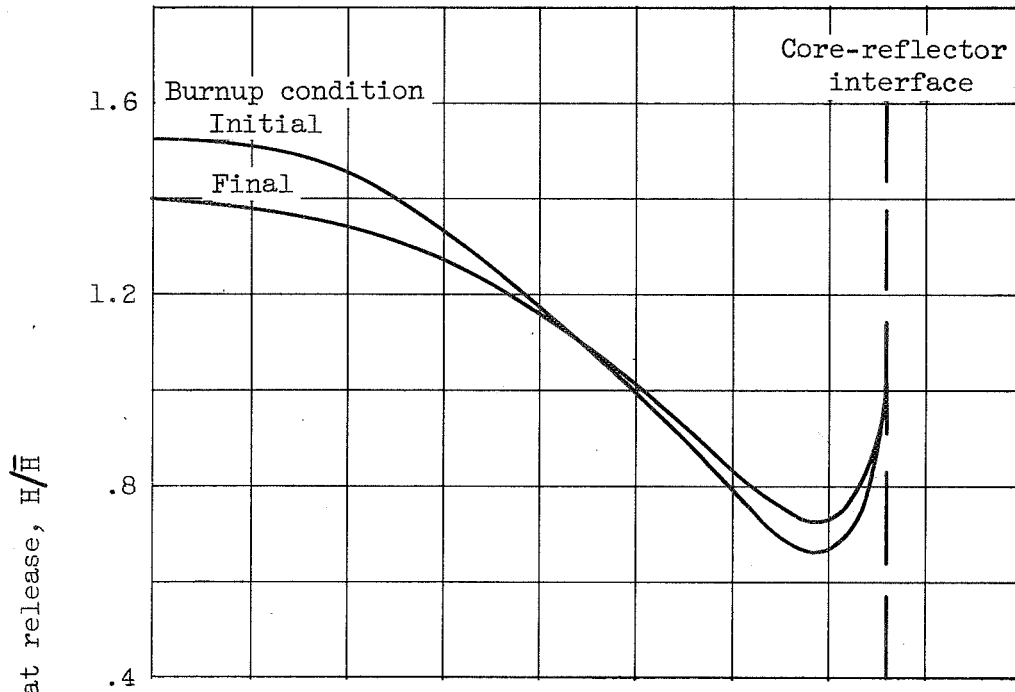
(c) Case SCW II.
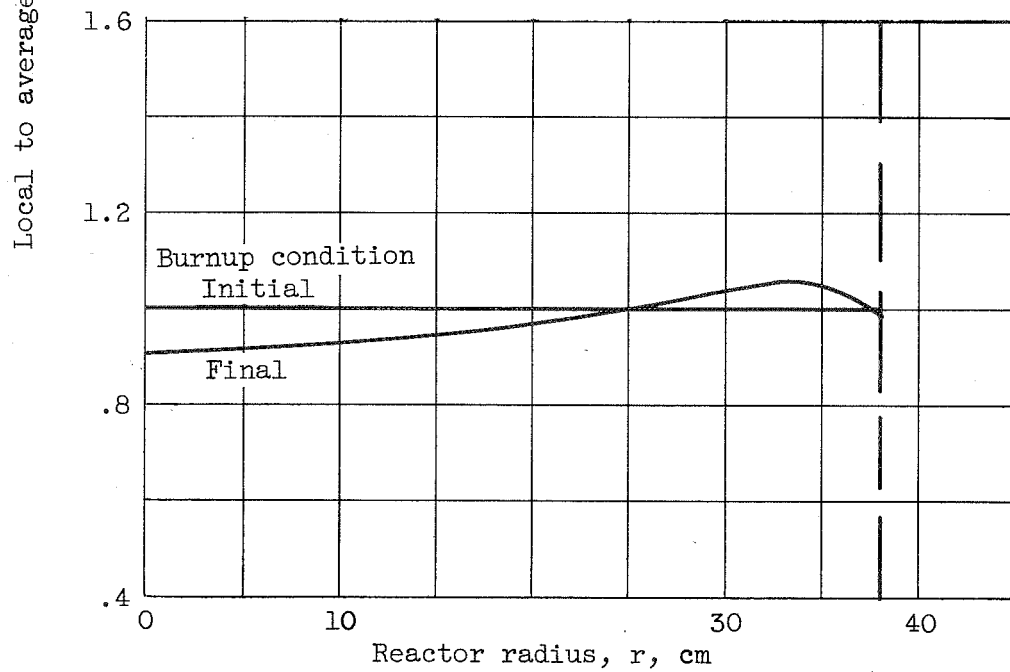
(d) Case SCW III.

Figure 2. - Concluded. Heat generation distributions.
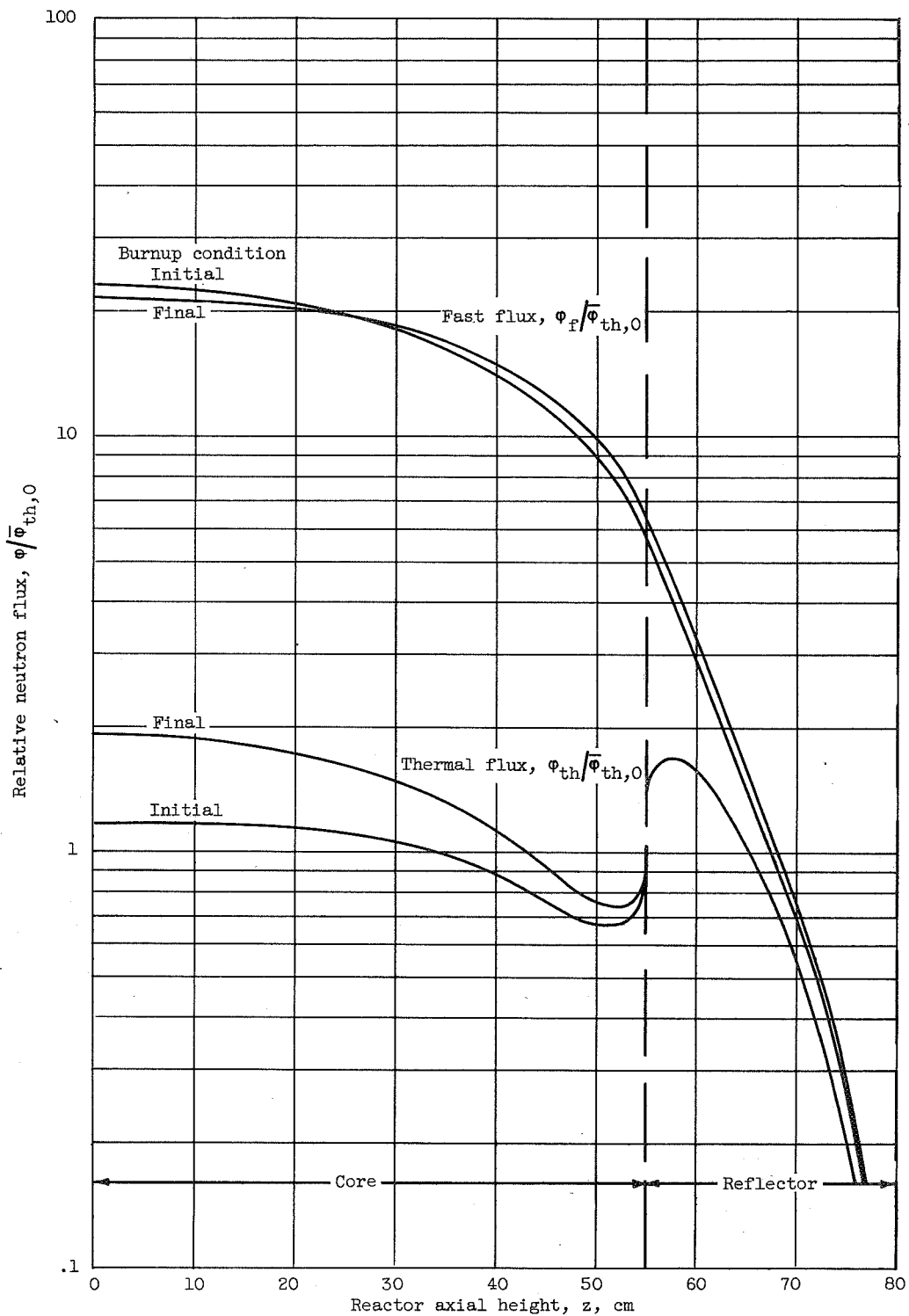
(a) Case SAR IV.

Figure 3. - Relative neutron flux distributions.
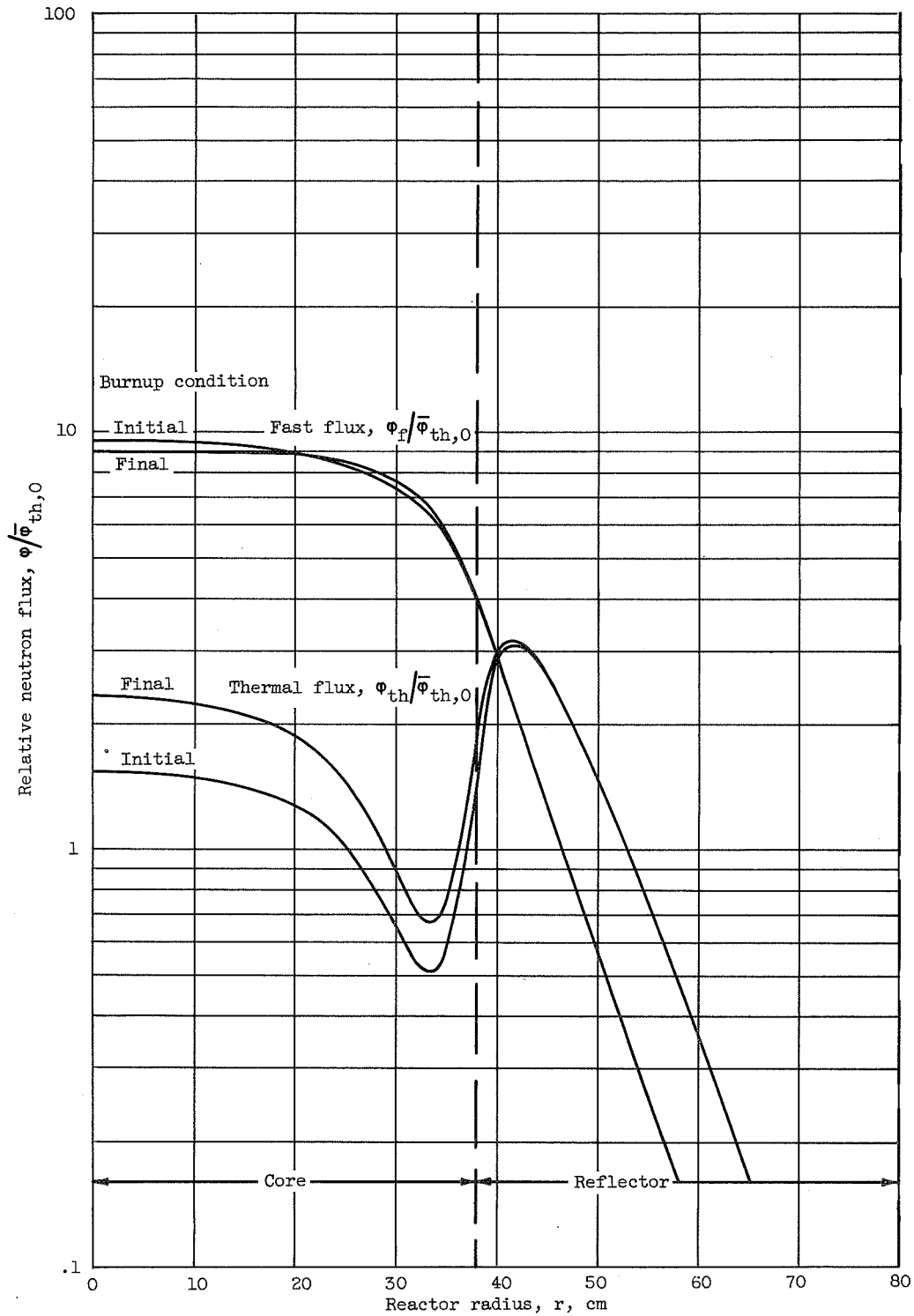
(b) Case SCW III.

Figure 3. - Concluded. Relative neutron flux distributions.
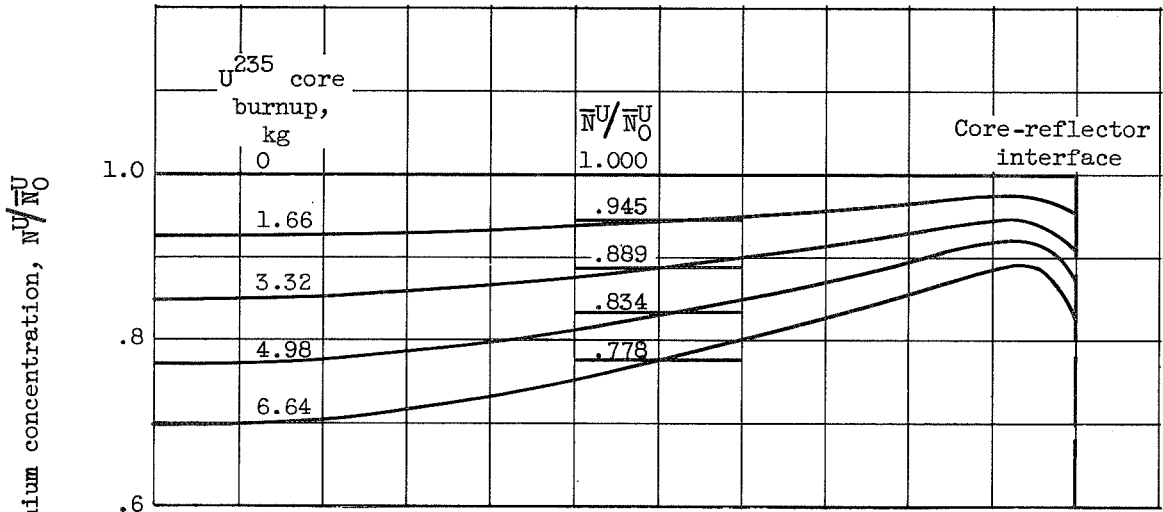
(a) Case SAR II.
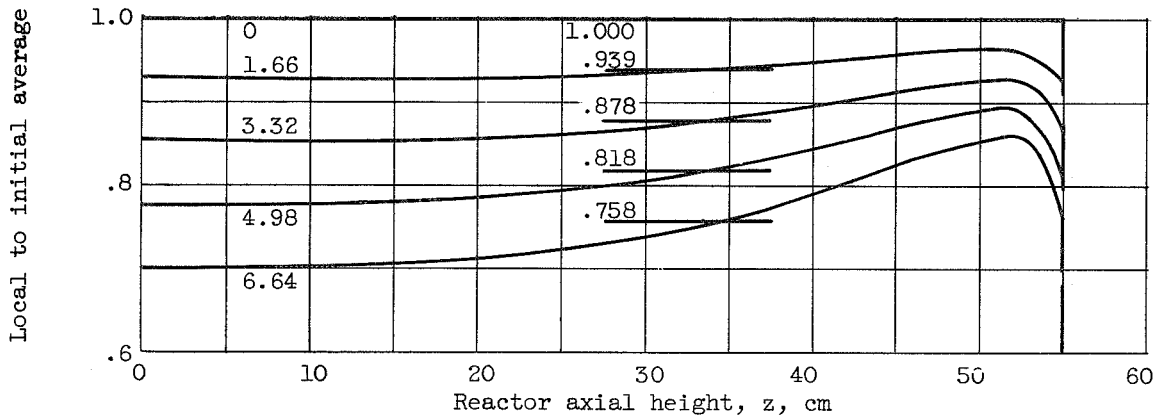
(b) Case SAR IV.

Figure 4. - Uranium-235 distributions.
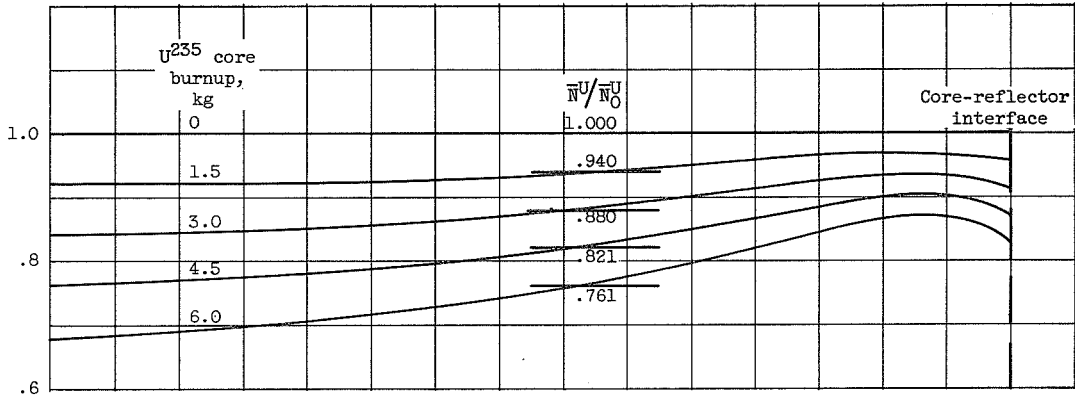
(c) Case SCW II.
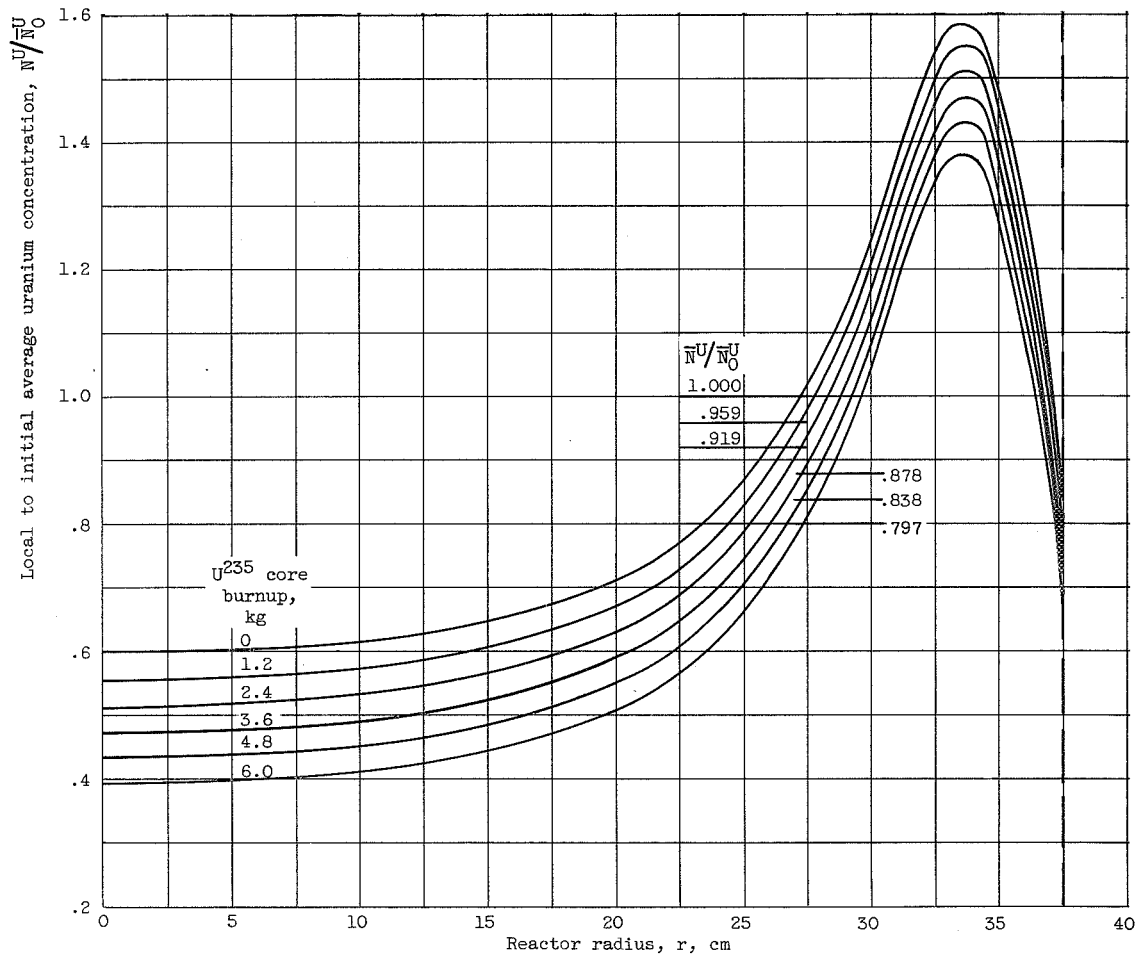
(d) Case SCW III.
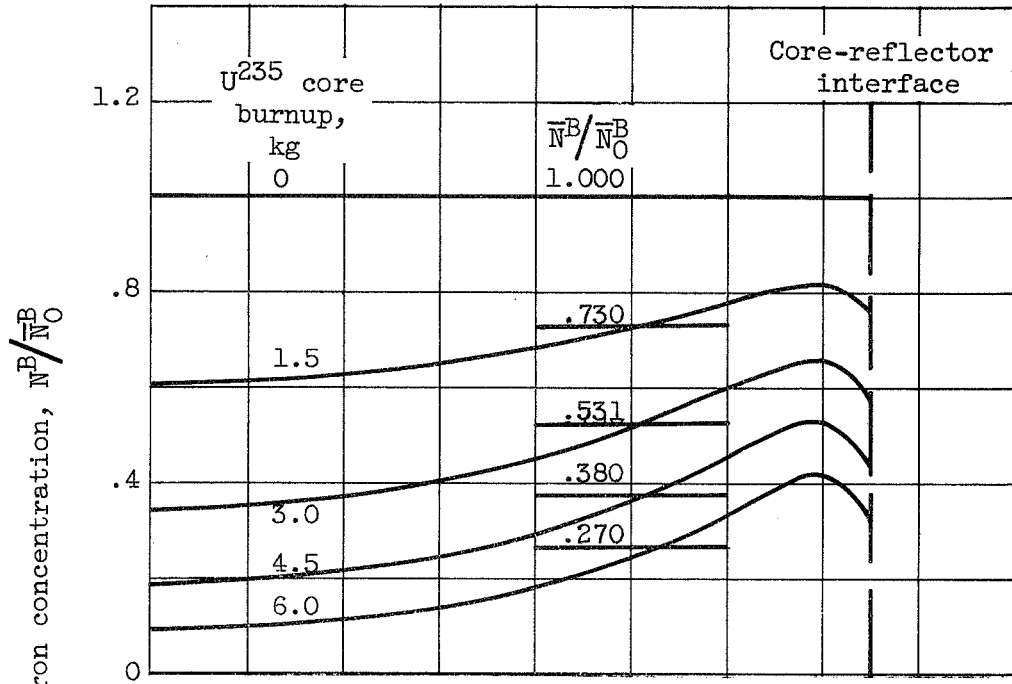
Figure 4. - Concluded. Uranium-235 distributions.
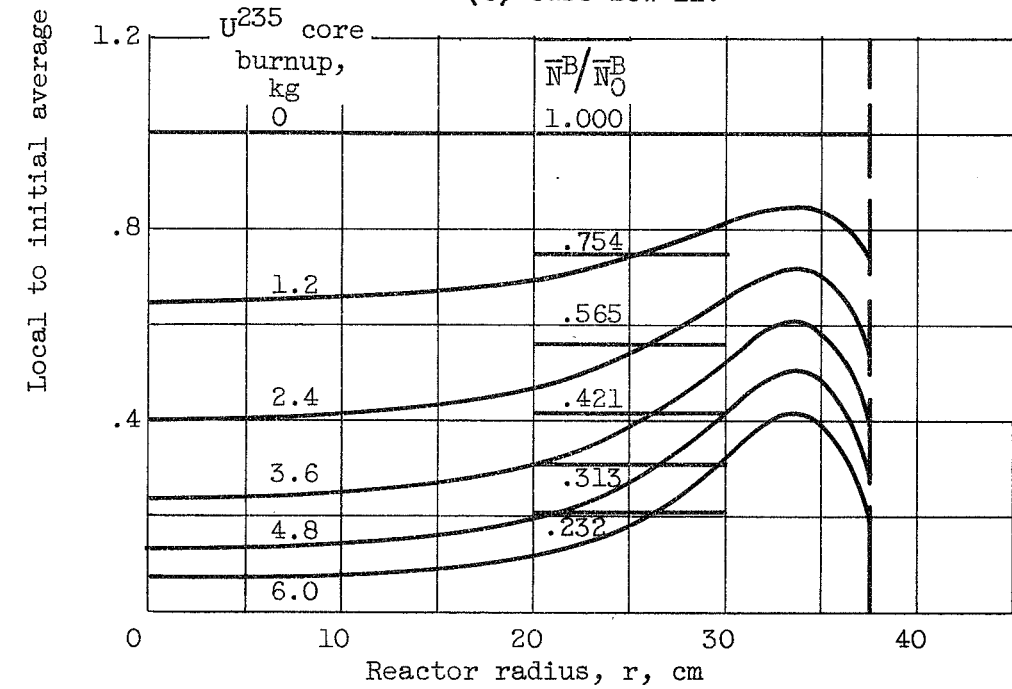
(a) Case SAR II.

(b) Case SAR IV.

Figure 5. - Boron-10 distributions.

SECRET

(c) Case SCW II.

(d) Case SCW III.
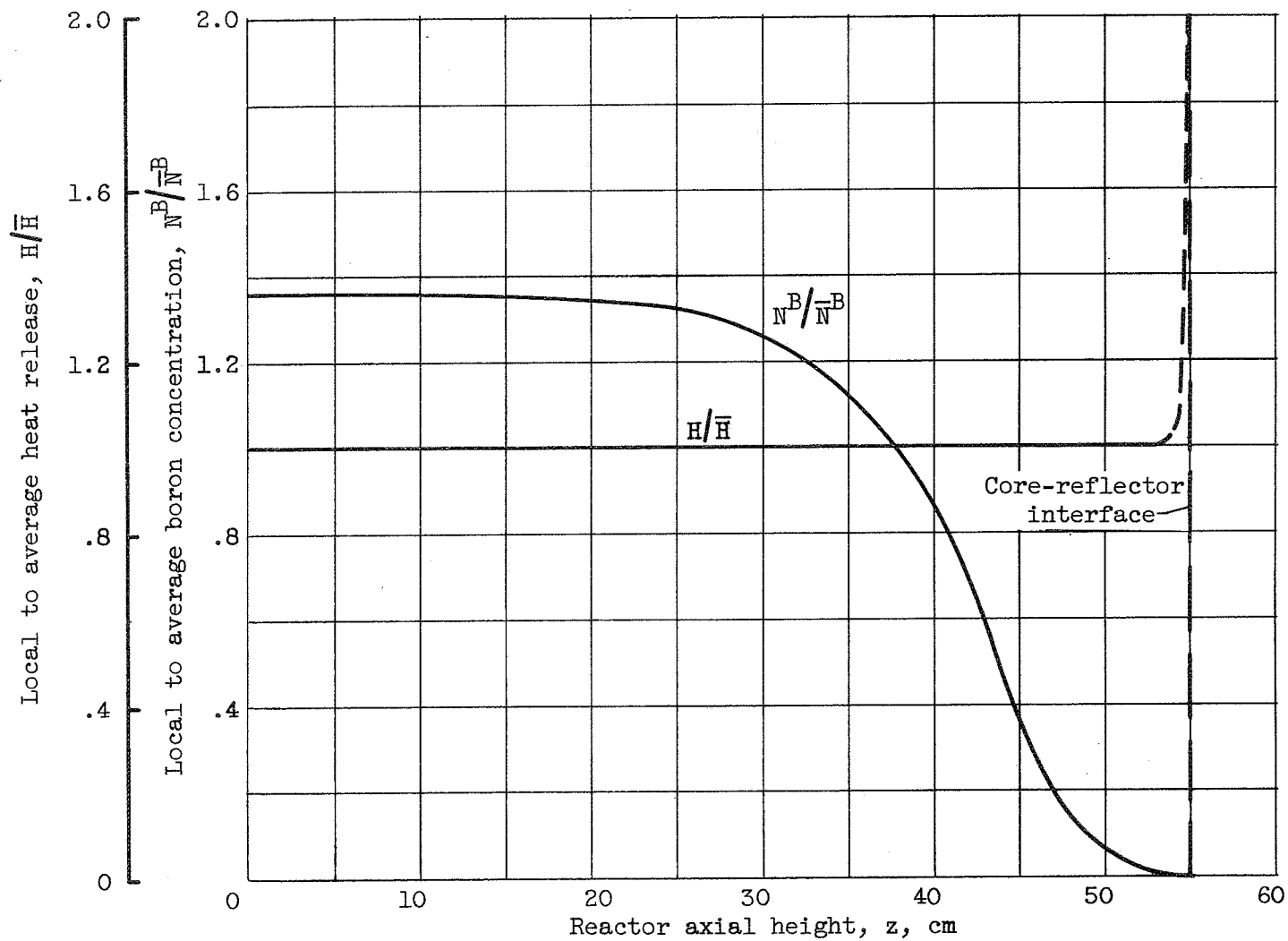
Figure 5. - Concluded. Boron-10 distributions.

Figure 6. - Startup boron distribution for initially uniform heat generation. SAR V.
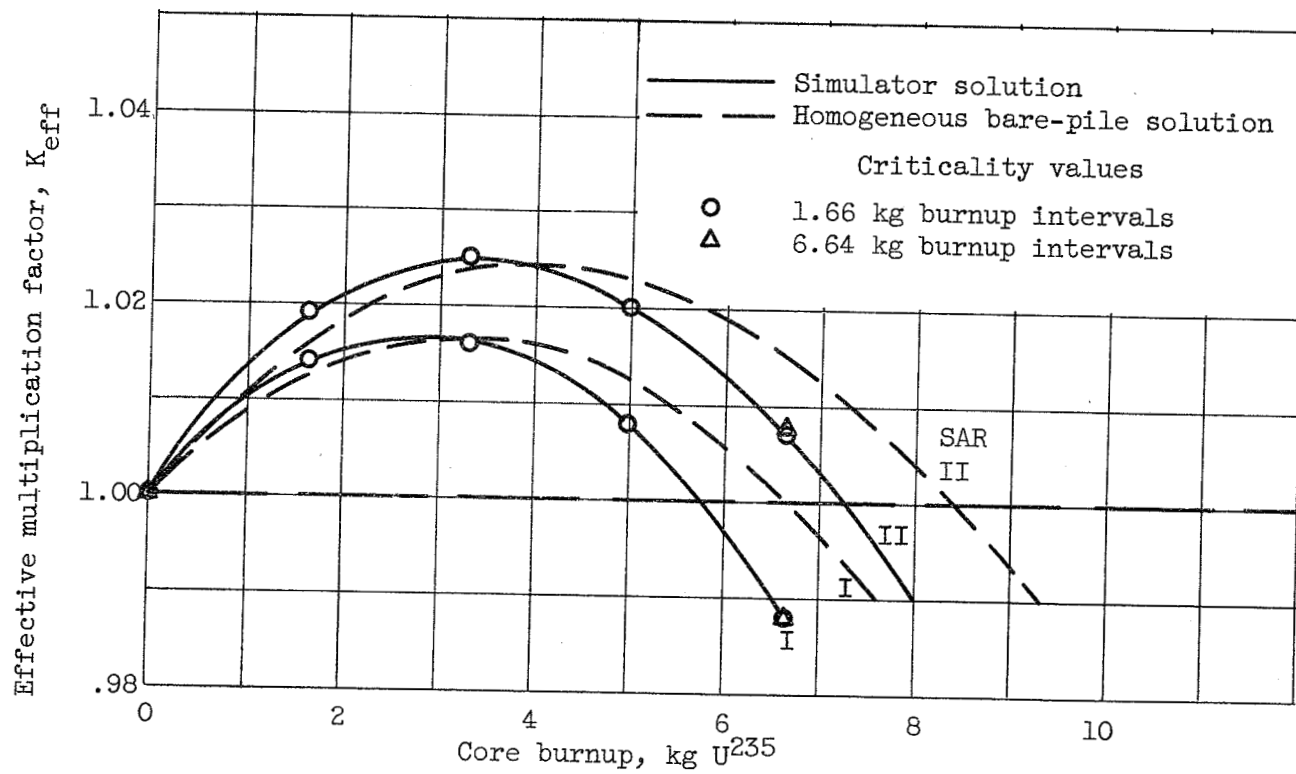
Figure 7. - Criticality variation with core uranium burnup.

Unclassified when detached from rest of report

Thomas A. Fox
Aeronautical Research Scientist
Propulsion Systems

Donald Bogart
Aeronautical Research Scientist
Propulsion Thermodynamics

Approved:

Leroy V. Humble
Aeronautical Research Scientist
Propulsion Thermodynamics

Benjamin Pinkel
Chief, Materials and Thermodynamics
Research Division

gah/3-23-55

~~CONFIDENTIAL~~ PRIORITY

NASA HEADQUARTERS

DKZ   6/7/72   9:00

EDWARD G. MAINES - SECURITY DIVISION   53356   X

NASA INSTALLATIONS
ATTN: SECURITY OFFICER

CONFIDENTIAL   NACA DOCUMENT RM E55C16, BY FOX AND BOGART WAS

ERRONEOUSLY LISTED AS UNCLASSIFIED BY HQS MEMO, 3/22/71, ITEM 7847

                                    L. # 213-23.   IF REASONABLY

                                        RIBUTED ON UNCLASSIFIED

SSLD TO CONFIDENTIAL R.D., GROUP L.   ADVISE OF SITUATIONS WHERE

RECOVERY NOT FEASIBLE.

EDWARD G. MAINES
NASA SECURITY CLASSIFICATION OFFICER

DISTRIBUTION:
AMES RESEARCH CENTER
FLIGHT RESEARCH CENTER
GODDARD SPACE FLIGHT CENTER
KENNEDY SPACE CENTER
LANGLEY RESEARCH CENTER
LEWIS RESEARCH CENTER
MANNED SPACECRAFT CENTER
MARSHALL SPACE FLIGHT CENTER
NASA PASADENA OFFICE
WALLOPS STATION

cc: KSS-10/RuDA

GROUP 4
...led at 3 year